Simulations of a compressible two-layer mixed-flows model with a staggered implicit scheme

Olivier Hurisse

Simulations of a compressible two-layer mixed-flows model with a staggered implicit scheme

O. Hurisse

olivier.hurisse@edf.fr, EDF Lab Chatou, 6 quai Watier, 78400 Chatou, France.

1 Introduction

The starting point of the present work is the model proposed in [1, 2, 3]. The latter has shown its capability to treat mixed flows of air and water in pipes with gravity effect. Very complex configurations such has pipe with a syphon have been tested with very satisfactory results. In a dynamical point of view, these situations are very close to those that are encountered when dealing with the phenomena of overspilling in inversed U-shaped tubes.

The compressible two-layer mixed-flows model (nicknamed CTL model in the following) is a two-fluid model which can be seen as an extension of the Baer-Nunziato model with isentropic phases (i.e. without energy equations). It is thus based on a mass balance equation and a momentum balance equation for each phase, supplemented by an equation on the height of liquid or the gas phase. A major difference with the Baer-Nunziato model arises in the definition of the non-conservative terms which are modified in order to account for the gravity. Obviously, relaxation source terms are different, but they are not considered in the present work.

In [1, 2, 3] efficient numerical schemes have been tested, mainly on the basis of fractional step approaches. The latter are very often used for the simulation of two-fluid models [5, 4, 6, 7]. One known drawback of these numerical techniques is that the underlying operator splitting implies a decoupling of the different physical effects. In some situations where these different effects strongly interact, this may leads to poor results on coarse meshes which are the targeted meshes for industrial applications. The aim of the present work is to test a numerical scheme that allows a complete coupling of all the physical effects. As a first step, source terms are not considered and we thus focus on the convective part of the CTL model proposed in [1, 2, 3].

The present document is organised as follow. The mathematical properties of the CTL model are not recalled here, on that point many details can be found in [1, 2, 3]. We thus begin in section 2 with the description of the numerical strategy: the algorithm for the time stepping is described in section 2.1 and the scheme used to approximate the spacial derivatives is detailed in section 2.2. In section 3, a verification test case is proposed and it allows to understand the behavior and the performance of the numerical scheme.

2 An implicit numerical scheme on staggered meshes

As mentioned in the introduction, we intend to develop a scheme that solves simultaneously all the physical effects. We have thus chosen an Euler implicit scheme for the time stepping. For this technique, it is required to solve a highly non-linear system which couples all the spacial degree of freedom at each time-step. Therefore, each time-step has a high CPU cost and, in order to limit the cost of whole simulation, the aim is then to limit this number of degree of freedom. It is thus mandatory to build a very accurate spacial discretization which can provides accurate approximations even on coarse meshes. This is the reason why we have chosen here to build the spacial discretization on staggered meshes, which are classically more accurate than schemes on co-located meshes. Obviously, the fact that we intend to simulate flows in one-dimensional pipes helps to make the choice of a staggered scheme.

Let us first recall the system of equations we are interested in, which models the configurations depicted by

figure 1:

$$\left\{\begin{array}{l} \partial_t\left(\alpha_2\right)+U_2\partial_x\left(\alpha_2\right)=0, \\ \partial_t\left(\alpha_1\rho_1\right)+\partial_x\left(\alpha_1\rho_1U_1\right)=0, \\ \partial_t\left(\alpha_1\rho_1U_1\right)+\partial_x\left(\alpha_1(\rho_1U_1^2+P_1(\rho_1))\right)-\mathcal{P}_I\partial_x\left(\alpha_1\right)=0, \\ \partial_t\left(\alpha_2\rho_2\right)+\partial_x\left(\alpha_2\rho_2U_2\right)=0, \\ \partial_t\left(\alpha_2\rho_2U_2\right)+\partial_x\left(\alpha_2(\rho_2U_2^2+P_2(\rho_2))\right)-\mathcal{P}_I\partial_x\left(\alpha_2\right)=0, \end{array}\right. \tag{1}$$

where we have $\alpha_1+\alpha_2=1$. The pressure $\mathcal{P}_I$ involved in the non-conservative terms are closed according to [1, 2, 3]:

$$\mathcal{P}_I=P_1(\rho_1)-\frac{g\alpha_1H\rho_1}{2},$$

and a pressure law $\rho_k\mapsto P_k(\rho_k)$ has to be provided for each phase. H corresponds to the total height and it is supposed constant and uniform here, see also figure 1. It should be noted that we consider here the case of a horizontal pipe, but that the model remains meaningful for non horizontal pipes with slope variations. System (1) is written using the set of non-conservative variables $Y=(\alpha_2,\rho1,U_1,\rho_2,U_2)$ gathering the following variables:

- α_1 which is the fraction of the total height occupied by phase 1, the remaining of the height given by α_2 being occupied by phase 2;
- ρ_k and U_k are respectively the density and the velocity of phase k.

An overview of the associated configurations can be found in figure 1.

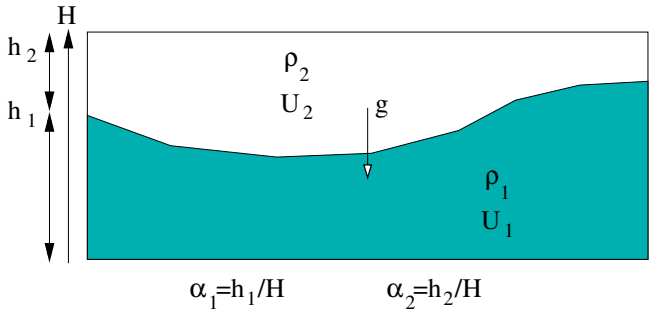

Figure 1: Configuration for the CTL model while considering horizontal pipes.

Let us also define the conservative variables $W=(\alpha_2,m_1,Q_1,m_2,Q_2)$ for which we have set: the partial masses $m_k=\alpha_k\rho_k$ and the momentum $Q_k=m_kU_k$. Considering the variables W, system (1) can be equivalently written:

$$\left\{\begin{array}{l} \partial_t\left(\alpha_2\right)+Q_2/m_2\ \partial_x\left(\alpha_2\right)=0, \\ \partial_t\left(m_1\right)+\partial_x\left(Q_1\right)=0, \\ \partial_t\left(Q_1\right)+\partial_x\left(Q_1^2/m_1+\alpha_1P_1(m_1/\alpha_1)\right)+\mathcal{P}_I(\alpha_1,m_1)\ \partial_x\left(\alpha_2\right)=0, \\ \partial_t\left(m_2\right)+\partial_x\left(Q_2\right)=0, \\ \partial_t\left(Q_2\right)+\partial_x\left(Q_2^2/m_2+\alpha_2P_2(\rho_2/\alpha_2)\right)-\mathcal{P}_I(\alpha_1,m_1)\ \partial_x\left(\alpha_2\right)=0, \end{array}\right. \tag{2}$$

The whole numerical scheme is based on system (2) and the conservative variable W. Such a choice make it more easy to ensure that numerical approximations fulfill balance relations for the mixture. Indeed, it is an important point to quote that since $\alpha_1+\alpha_2=1$, system (2) (and obviously system (1)) leads to a balance equation for the total mass (m_1+m_2) and for the total momentum (Q_1+Q_2).

2.1 An implicit time-stepping

We propose here to use an implicit time-stepping algorithm for system (2). The simplest choice is to use an Euler scheme. In order to describe some properties of the scheme, let us write system (2) in a more convenient and compact form:

$$\partial_t\left(W\right)+\partial_x\left(F(W)\right)+C(W)\partial_x\left(W\right)=0, \tag{3}$$

with

$$F(W)=(0,Q_1,Q_1^2/m_1+\alpha_1P_1,Q_2,Q_2^2/m_2+\alpha_2P_2)\quad\text{and}\quad C(W)=(Q_2/m_2,0,\mathcal{P}_I,0,-\mathcal{P}_I).$$

When considering an approximated solution W^n of the solution at time t^n, the implicite Euler scheme for (3) gives the following update formula for the approximated solution W^{n+1} of the solution at time $t^{n+1} = t^n + \Delta t$:

$$W^{n+1} = W^n - \Delta t \ \left(\partial_x \left(F(W^{n+1})\right) - C(W^{n+1})\partial_x \left(W^{n+1}\right)\right). \tag{4}$$

Computing W^{n+1} thus requires to solve a non-linear system. Using a Newton or quasi-Newton method to solve (4) may be tricky. Hopefully, it should be noted from relation (4) that W^{n+1} is a fix point for the function $W^{n+1} \mapsto \mathcal{F}(W^{n+1})$ with:

$$\mathcal{F}(W^{n+1}) = W^n - \Delta t \ \left(\partial_x \left(F(W^{n+1})\right) - C(W^{n+1})\partial_x \left(W^{n+1}\right)\right).$$

It seems then quite natural to solve (4) by the mean of the Picard's method. The latter has the advantage to be easily implemented and to avoid the computation of approximations of the derivatives of system (4), which may become very complex and costly. Nevertheless, in order to converge the Picard's method required to be applied on a contracting mapping. This condition can be fulfilled by the function $\mathcal{F}$ for small enough time step Δt.

Let us exhibit, at less formally if not rigorously, such constraint on the time-step. When considering regular solutions, function $\mathcal{F}$ reads:

$$\mathcal{F}(W^{n+1}) = W^n - \Delta t \ A(W^{n+1})\partial_x \left(W^{n+1}\right),$$

where $A(W) = \partial_W \left(F(W)\right) + C(W)$ is the convection matrix of system (3). Therefore for two sets of variables Z_a and Z_b, we have:

$$\mathcal{F}(Z_b) - \mathcal{F}(Z_a) = -\Delta t \ \left(A(Z_b)\partial_x \left(Z_b\right) - A(Z_a)\partial_x \left(Z_a\right)\right)$$

Formally, using a Taylor expansion leads to:

$$\mathcal{F}(Z_b) - \mathcal{F}(Z_a) = -\Delta t \ A(Z_a)\partial_x \left(Z_b - Z_a\right) - \Delta t \ \partial_Z \left(A(Z_a)\right)\left(Z_b - Z_a\right)\partial_x \left(Z_a\right) + \Delta t \ o(|Z_b - Z_a|).$$

We now assume that the spatial derivatives in function $\mathcal{F}$ are approximated through a first order formula with respect to a space size Δx. Moreover, since we are dealing with regular solutions, we assume that Z_a and Z_b, are such that $Z_b = Z_a + o(\Delta x)$. We then get that $\Delta x \ \partial_x \left(Z_a\right) = Z_b - Z_a + o(\Delta x)$ and thus:

$$\mathcal{F}(Z_b) - \mathcal{F}(Z_a) = -\frac{\Delta t}{\Delta x} A(Z_a)(Z_b - Z_a) + o(1).$$

Therefore, a sufficient condition for $\mathcal{F}$ to be a contraction mapping in those conditions is:

$$\frac{\Delta t}{\Delta x}\lambda(A(Z_a)) < 1, \tag{5}$$

where $\lambda(A(Z_a))$ is the spectral radius of A. We recover here a classical CFL condition for explicit schemes based on the whole set of the wave speed of the system, and thus based on the pressure wave speed. In our case, this constraint arises from a requirement of the Picard's method. It is not clear if such a condition would be necessary when using a Newton method for solving (4). With such kind of algorithm, such a CFL condition could be hidden in the fact that the starting point of the (quasi-)Newton's methods must be in the neighborhood of the solution (for instance if the result of the previous iterate is used as a starting point).

The CFL condition above has been exhibited considering regular solutions. In our practical experiments, we have set:

$$\Delta t < \left(\max_i(\lambda(A(W_i^n))\right)^{-1} \Delta x/2, \tag{6}$$

where W_i^n is the approximated value in cell i at the beginning of the iteration $n \to n+1$, i.e. at time t^n. It seems to allow the convergence of the Picard's method even for solutions involving shock waves.

2.2 Spacial discretisation on staggered meshes

The spatial derivatives in system (4) are approximated using a first order finite volume scheme on staggered meshes. We consider that the primal mesh is associated with the "thermodynamical" quantities: α_2 and m_k, whereas the dual mesh is associated with the momentums Q_k. Cell i of the primal mesh is the interval $[x_i, x_{i+1}]$ with $x_{i+1} = x_i + L_i$. Then cell i of the dual mesh is "centered" on the left boundary of the cell i of the primal mesh: it corresponds to the interval $[x_i - L_{i-1}/2, x_i + L_i/2]$, which has thus a length $\widetilde{L}_i = L_{i-1}/2 + L_i/2$. We also define the following mean quantities on the cell i of the primal mesh:

$$\alpha_{k,i}^{n+1} = \frac{1}{L_i}\int_{x_i}^{x_{i+1}} \alpha_k^{n+1}(x)dx, \quad \text{and} \quad m_{k,i}^{n+1} = \frac{1}{L_i}\int_{x_i}^{x_{i+1}} m_k^{n+1}(x)dx,$$

and on cell i of the dual mesh:

$$Q_{k,i}^{n+1} = \frac{1}{\widetilde{L}_i} \int_{x_i - L_{i-1}/2}^{x_i + L_i/2} Q_k^{n+1}(x) dx.$$

A sketch of all these notations is proposed in figure 2.

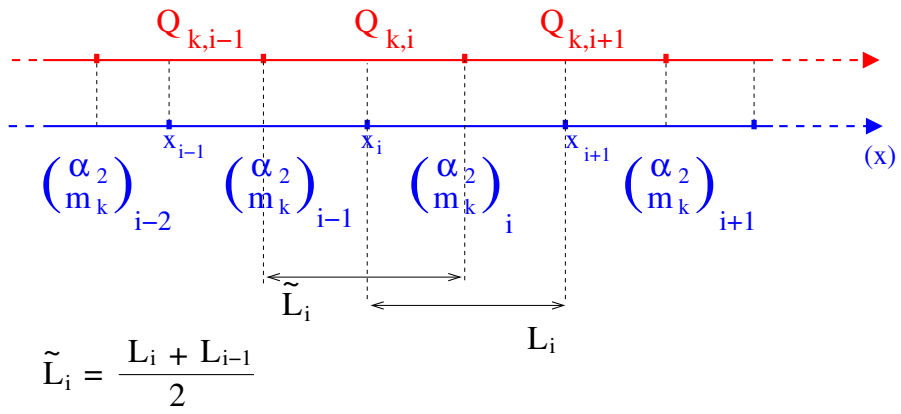

Figure 2: Notations and settings of the staggered meshes: the primal mesh is in blue, and the dual mesh is in red.

The main advantage of such meshes when considering finite volume schemes is that the mass equations are easily written in a discrete form. Indeed, the natural manner for discretizing the mass equations is:

$$m_{k,i}^{n+1} = m_{k,i}^{n} - \frac{\Delta t}{L_i} \left(Q_{k,i+1}^{n+1} - Q_{k,i}^{n+1} \right). \tag{7}$$

On the contrary, in the equations for α_2 and for the momentums, quantities defined on both the primal and the dual meshes are combined in the fluxes. The discretization of these equations thus requires interpolations of some quantities. Obviously, many different consistent interpolations may be proposed, leading to different schemes. In the sequel, we propose to use for the fraction α_2 a scheme that is close to the Lax-Friedrichs method adapted to the non-conservative case:

$$\alpha_{2,i}^{n+1} = \alpha_{2,i}^{n} - \frac{\Delta t}{L_i} \widetilde{U}_{2,i}^{n+1} \delta\widetilde{\alpha}_{2,i}^{n+1} - \Delta t \frac{\widetilde{L}_i + \widetilde{L}_{i+1}}{2} \left(\frac{\alpha_{2,i+1}^{n+1} - \alpha_{2,i}^{n+1}}{\widetilde{L}_{i+1}} - \frac{\alpha_{2,i}^{n+1} - \alpha_{2,i-1}^{n+1}}{\widetilde{L}_i} \right), \tag{8}$$

where the upwind part of the update uses the interpolated velocity:

$$\widetilde{U}_{2,i}^{n+1} = \frac{Q_{2,i+1}^{n+1} + Q_{2,i}^{n+1}}{2\ m_{2,i}^{n+1}},$$

and the quantity:

$$\delta\widetilde{\alpha}_{2,i}^{n+1} = \begin{cases} \alpha_{2,i}^{n+1} - \alpha_{2,i-1}^{n+1}, & \text{if} \quad \widetilde{U}_{2,i}^{n+1} > 0, \\ \alpha_{2,i+1}^{n+1} - \alpha_{2,i}^{n+1}, & \text{otherwise.} \end{cases}$$

The momentum equations are discretized following the formula:

$$\begin{aligned} Q_{k,i}^{n+1} = Q_{k,i}^{n} \quad & - \quad \frac{\Delta t}{\widetilde{L}_i} \left(\frac{E_{c,i,+}^{n+1}}{m_{k,i}^{n+1}} + \alpha_{k,i}^{n+1} P_k(m_{k,i}^{n+1}/\alpha_{k,i}^{n+1}) - \frac{E_{c,i,-}^{n+1}}{m_{k,i-1}^{n+1}} - \alpha_{k,i-1}^{n+1} P_k(m_{k,i-1}^{n+1}/\alpha_{k,i-1}^{n+1}) \right) \\ & - \quad -\frac{\Delta t}{\widetilde{L}_i} \widetilde{\Pi}_i^{n+1} (\alpha_{k,i}^{n+1} - \alpha_{k,i-1}^{n+1}), \end{aligned} \tag{9}$$

where $E_{c,i,+}^{n+1}$ and $E_{c,i,-}^{n+1}$ are upwind kinetic energies defined as:

$$E_{c,i,+}^{n+1} = \begin{cases} Q_{k,i}^{n+1}, & \text{if} \quad \widetilde{Q}_{k,i,+}^{n+1} = \frac{Q_{k,i+1}^{n+1} + Q_{k,i}^{n+1}}{2} > 0, \\ Q_{k,i+1}^{n+1}, & \text{otherwise;} \end{cases}$$

and

$$E_{c,i,-}^{n+1} = \begin{cases} Q_{k,i-1}^{n+1}, & \text{if} \quad \widetilde{Q}_{k,i,-}^{n+1} = \frac{Q_{k,i}^{n+1}+Q_{k,i-1}^{n+1}}{2} > 0, \\ Q_{k,i}^{n+1}, & \text{otherwise.} \end{cases}$$

The pressure term $\widetilde{\Pi}_i^{n+1}$ arising in the discretized counterpart of the non-conservative product is defined as:

$$\widetilde{\Pi}_i^{n+1} = \frac{P_1(m_{1,i}^{n+1}/\alpha_{1,i}^{n+1}) + P_1(m_{1,i-1}^{n+1}/\alpha_{1,i-1}^{n+1})}{2} - \frac{gH}{2}\frac{L_i m_{1,i}^{n+1} + L_{i-1} m_{1,i-1}^{n+1}}{L_i + L_{i-1}}.$$

At this point, equations (7), (8) and (9) are the equations to be solved in order to compute the approximated value W^{n+1}. It should be mentioned that the associated function $\mathcal{F}$ defined in the previous section 2.1 is not continuous because of the upwind terms introduced in equations (8) and (9). Neverthless, it seems that it does not avoid the Picard's method to behave correctly in our numerical experiments when considering the CFL condition (6) for the time step Δt.

3 Verification test case

We propose in this section to test the numerical method described in section 2 on a Riemann problem involving only shocks and a contact discontinuity. A very similar test case was used in [1, 2, 3]. The wave configuration of this Riemann problem is depicted in figure 3. As in [1, 2, 3], we consider here a linear law for phase 1 and a perfect gas law for phase 2:

$$P_1(\rho_1) = C_{1,ref}^2(\rho_1 - \rho_{1,ref}) + P_{1,ref},$$

$$\text{with} \quad C_{1,ref} = 1500\ m/s, \quad \rho_{1,ref} = 998.1115\ kg/m^3, \quad P_{1,ref} = 1.0133e5\ Pa;$$

$$P_2(\rho_2) = P_{2,ref}\left(\frac{\rho_2}{\rho_{2,ref}}\right)^{\gamma_2},$$

$$\text{with} \quad P_{2,ref} = 1.01325e5\ Pa, \quad \rho_{2,ref} = 1.204\ kg/m^3, \quad \gamma_2 = 1.4.$$

The total height H is set to 1. The intermediate states Y_m, $m \in \{1, 2, 3, 4\}$, Y_L and Y_R, defining the Riemann problem considered here are gathered in table 1. We consider the final time $t_{end} = 2.3\ 10^{-3}\ s$. Convergence curves are plotted in figure 4 for meshes containing from 100 to 200000 cells. It should be noted from figure 4 that we almost recover the expected asymptotic rate of convergence of 1/2 for α_2, ρ_1 and Q_1. The variables ρ_2 and Q_2 still present an convergence rate slightly greater than 1/2, even for the finest meshes. The approximated solution obtained for a mesh containing 1000 cells is plotted in figure 5.

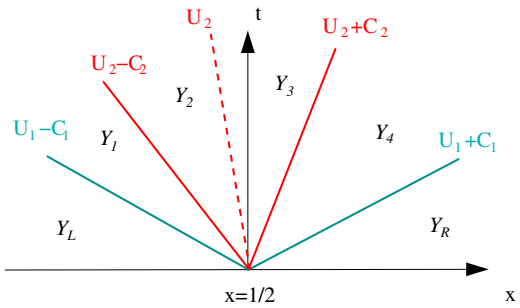

Figure 3: Configuration of the different waves for the Riemann problem: $U_k \pm c_k$-waves are shocks whereas the U_2-wave is obviously a contact discontinuity. The initial discontinuity between left and right states, respectively Y_L and Y_R, is located at $x = 1/2$.

	α_2	$\rho_1\ (kg/m^3)$	$U_1\ (m/s)$	$\rho_2\ (kg/m^3)$	$U_2\ (m/s)$
Y_L	0.5	998.111500000000	10	1.204	5
Y_1	0.5	998.161101784576	9.9254584	1.204	5
Y_2	0.5	998.161101784576	9.9254584	1.26422702503085	−11.83896
Y_3	0.4976253	998.16208780496	9.82255768821687	1.26012920420671	−11.83896
Y_4	0.4976253	998.16208780496	9.82255768821687	1.23491558633234	−18.826134
Y_R	0.4976253	998.062877627989	9.673461	1.23491558633234	−18.826134

Table 1: Intermediate states for the Riemann problem.

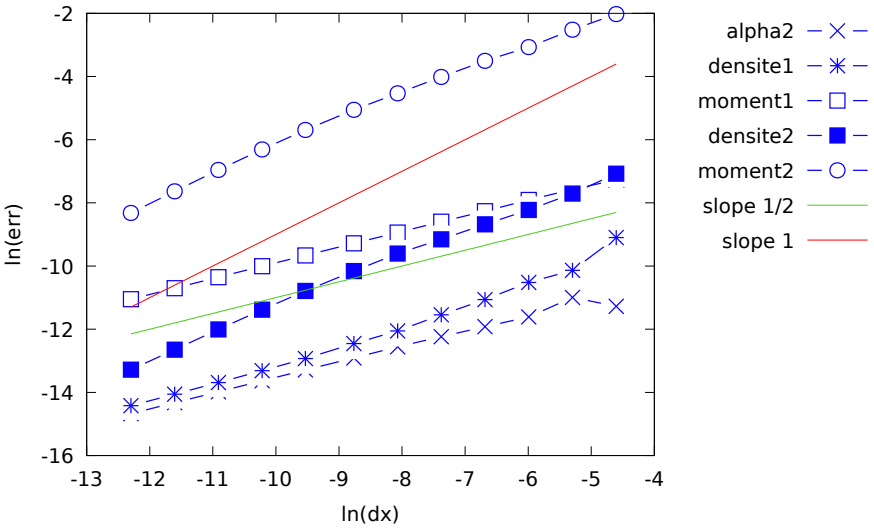

Figure 4: Convergence curves for meshes containing from 100 to 200000 cells.

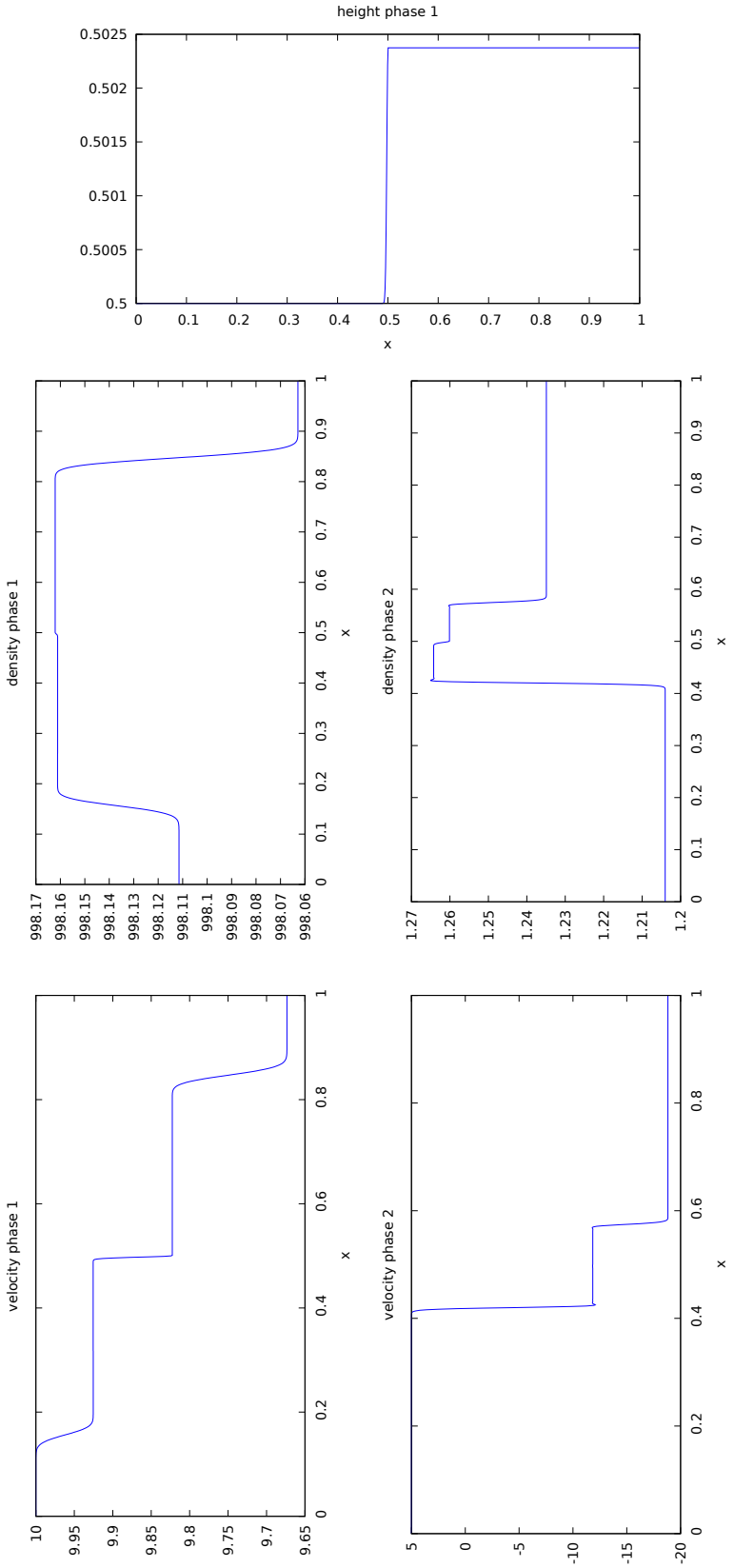

Figure 5: Results for ρ_k and U_k for a mesh with 1000 cells.

References

[1] Charles Demay. Modelling and simulation of transient air-water two-phase flows in hydraulic pipes. *These, Université Grenoble Alpes, tel.archives-ouvertes.fr/tel-01651078v3*, 2017.

[2] Charles Demay, Christian Bourdarias, Benoît de Laage de Meux, Stéphane Gerbi, and Jean-Marc Hérard. Numerical simulation of a compressible two-layer model: A first attempt with an implicit–explicit splitting scheme. *Journal of Computational and Applied Mathematics*, 346:357–377, 2019.

[3] Charles Demay and Jean-Marc Hérard. A compressible two-layer model for transient gas–liquid flows in pipes. *Continuum Mechanics and Thermodynamics*, 29(2):385–410, 2017.

[4] Jean-Marc Hérard and Olivier Hurisse. Computing two-fluid models of compressible water-vapour flows with mass transfer. In *42nd AIAA Fluid Dynamics Conference and Exhibit, AIAA paper 2012-2959*, 2012.

[5] Jean-Marc Hérard and Olivier Hurisse. A fractional step method to compute a class of compressible gas–liquid flows. *Computers & Fluids*, 55:57–69, 2012.

[6] Yujie Liu. *Contribution to the verification and the validation of an unsteady two-phase flow model*. Theses, Aix-Marseille Université, September 2013.

[7] H Lochon. *Modélisation et simulation d'écoulements transitoires eau-vapeur*. PhD thesis, PhD thesis, Aix-Marseille, 2016.